Article

Not peer-reviewed version

Redox Metabolism and Vascular Calcification in Chronic-Kidney Disease

Cristina Alonso-Montes [‡], Natalia Carrillo-López [‡], Sara Panizo [‡], Beatriz Martín-Carro, Juan Carlos Mayo Barrallo, Pablo Román-García, Raúl García-Castro, Jesús M. Fernández-Gómez, Miguel A. Hevia-Suárez, Julia Martín-Vírgala, Sara Fernández-Villabrille, Laura Martínez-Arias, Sara Barrio Vázquez, Laura Calleros Basilio, Jorge Benito Cannata-Andía [*], Manuel Naves-Díaz [*], José Luis Fernández-Martín [†], Isabel Quirós-González [*,†]

Posted Date: 26 July 2023

doi: 10.20944/preprints202307.1684.v1

Keywords: Vascular calcification; Catalase; CKD; RUNX2; Epigastric arteries; DIGE

Article

Redox Metabolism and Vascular Calcification in Chronic-Kidney Disease

Cristina Alonso-Montes [1,2,‡], Natalia Carrillo-López [1,2,‡], Sara Panizo García [1,2,‡], Beatriz Martín-Carro [1,2], Juan Carlos Mayo Barrallo [3], Pablo Román-García [1], Raúl García-Castro [4], Jesús María Fernández-Gómez [5,6], Miguel Ángel Hevia-Suárez [5,6], Julia Martín-Vírgala [1,2], Sara Fernández-Villabrille [1,2], Laura Martínez-Arias [1,2], Sara Barrio Vázquez [1], Laura Calleros Basilio [2,7], Jorge Benito Cannata-Andía [1,2,8,*], Manuel Naves-Díaz [1,2,*], José Luis Fernández-Martín [1,2,†] and Isabel Quirós-González [3,†,*]

[1] Bone and Mineral Research Unit, Hospital Universitario Central de Asturias, Instituto de Investigación Sanitaria del Principado de Asturias (ISPA), Oviedo, Spain; cristinaam.huca@gmail.com (C.A.M.); ncarrillolopez.huca@gmail.com (N.C.L.); sarapanizogarcia@gmail.com (S.P.G.); bea_m15@hotmail.com (B.M.C.); pablo.roman.garcia@gmail.com (P.R.G.); julia.martinvirgala90@gmail.com (J.M.V.); sarafv0012@gmail.com (S.F.V.); lauramartinezarias@gmail.com (L.M.A.); sbarriovazquez@gmail.com (S.B.V.); jorge.cannata@gmail.com (J.B.C.A.); mnaves.huca@gmail.com (M.N.D.); jlfernandez.huca@gmail.com (J.L.F.M.)

[2] Redes de Investigación Cooperativa Orientadas a Resultados en Salud (RICORS), RICORS2040 (Kidney Disease), Madrid, Spain

[3] Department of Cellular Morphology and Biology, Instituto Universitario de Oncologia del Principado de Asturias (IUOPA), Universidad Oviedo, Instituto de Investigación Sanitaria del Principado de Asturias (ISPA), Oviedo, Spain; mayojuan@uniovi.es (J.C.M.B.); iquirosg@gmail.com (I.Q.G.)

[4] Department of Nephrology. Hospital Juaneda Miramar. Red Asistencial Juaneda. Palma de Mallorca, Spain; rgccandanedo@gmail.com (R.G.C.)

[5] UGC of Urology, Hospital Universitario Central de Asturias, University of Oviedo Oviedo, Spain; jmfernandezgomez23@gmail.com (J.M.F.G.); hevia.urologo@gmail.com (M.A.S.H.)

[6] Department of Surgery and Medical Surgical Specialities, Universidad de Oviedo, Oviedo, Spain.

[7] Department of Systems Biology, Physiology Unit, Universidad de Alcalá, Alcalá de Henares, Spain.; laura.calleros@edu.uah.es (L.C.B.)

[8] Department of Medicine, Universidad de Oviedo, Oviedo, Spain

* Correspondence: jorge.cannata@gmail.com (J.B.C.A.); mnaves.huca@gmail.com (M.N.D.); iquirosg@gmail.com (I.Q.G.)

† These authors contributed equally to this work.

‡ These authors contributed equally to this work.

Abstract: Vascular calcification (VC), is a common complication in patients with chronic kidney disease and increases mortality. Although oxidative stress is involved in the onset and progression of this disorder, the specific role of some main redox regulators such as catalase, the main scavenger of H_2O_2, remains unclear. In the present study, epigastric arteries of kidney transplant recipients, an *in vivo* model of VC and an *in vitro* model of VC exhibiting catalase overexpression (Cts) were analyzed. Peri-calcification areas of human epigastric arteries have increased levels of catalase and cytoplasmic rather than nuclear RUNX2. In the *in vivo* model, advanced aortic VC concurs with lower levels of the H_2O_2 scavenger, glutathione peroxidase 3 compared to controls. In an early model of calcification using vascular smooth muscle cells (VSMCs), Cts VSMCs showed the expected increase in RUNX2 total levels. However, Cts VMSC also exhibited lower percentage of the nucleus stained for RUNX2 in response to calcifying media. At this early model of VC we did not observe dysregulation of mitochondrial redox state, an increase in general redox state was observed in the cytoplasm. These *in vivo* and *in vitro* results highlight the complex role of antioxidant enzymes as catalase in the process of VC by regulation of RUNX2 location.

Keywords: vascular calcification; catalase; CKD; RUNX2; epigastric arteries; DIGE

 doi:10.20944/preprints202307.1684.v1

1. Introduction

Vascular calcification (VC) is one of the most common co-morbidities associated with Chronic Kidney Disease (CKD) [1]. CKD is defined as kidney damage associated to a reduction of the glomerular filtration rate for at least 3 months [2]. The loss of renal function affects serum biochemical levels of calcium, phosphorus, alkaline phosphatase and parathormone (PTH), having a progressive serious impact on vascular, heart, bone and parathyroid gland functions [1,3]. VC results as a deposition of hydroxyapatite crystals in the medial or intima layers of arteries. It is a complex process that includes redox alterations, cell reprogramming, inflammation and extracellular matrix degradation among others [4]. Incidence of VC increases progressively during CKD [5] although there is some individual propensity whose causes remains unclear [3].

Redox species are one of the main mediators of cell signalling, homeostasis and metabolism. Among reactive oxygen species (ROS), hydrogen peroxide (H_2O_2) is an effective secondary messenger that can diffuse to different cell compartments and the extracellular space [6]. In the context of vascular tissue, there are two redox metabolites essential for vascular homeostasis, nitric oxide which acts mainly at endothelium level [7] and H_2O_2 which regulates proliferation, differentiation and contractility of vascular smooth muscle cells (VSMCs) of the media layer [8]. ROS have to be contained in specific cell compartments and within the beneficial range of concentration (oxidative eustress) by antioxidant molecules (i.e. glutathione, GSH), and antioxidant enzymes, such as GSH peroxidases or catalase that have specific locations to perform their functions [6]. In pathological conditions this balance favours ROS production causing deleterious effects (oxidative distress).

In VSMCs this distress causes VC, increased levels of H_2O_2 alone have been shown to induce VC in VSMC through the osteogenic transcription factor Runx2 [9]. In addition, it has been shown a protective effect of various antioxidants against calcium and phosphorus induced VC [10]. Catalase is the most effective H_2O_2 scavenging enzyme and catalase polymorphism are associated with prevention of arterial aging [11]. However, there are very few studies about their implication in cardiovascular disease or in CKD [12,13] and their results were inconclusive. A recent report has shown a potential protective role of catalase in VC [14]; the following work examines the role of redox metabolism in VC associated to CKD (VC-CKD).

2. Materials and Methods

2.1. Kidney transplant recipient clinical data and epigastric arteria collection

Epigastric arteries were collected from kidney transplant recipients (N= 17). A section of epigastric artery was fixed in formaldehyde 4% and embedded in paraffin for immunohistochemistry analysis. Clinical data including demographic characteristics (sex, age, smoking status and body mass index), comorbidities (hypertension and hyperlipidaemia), treatments (time on dialysis), and biochemical parameters (serum phosphate and calcium) at the time of transplant were collected. All patients provided their informed consent to participate. The study was conducted according to the principles of Helsinki and approved by the Research Ethics Committee of the Principality of Asturias.

2.2. Experimental model in vivo: establishment of vascular calcification in Wistar rats

The *in vivo* study was performed according a previously described model to induce VC [15,16]. Briefly, in 18 four months old male Wistar rats, chronic renal failure (CRF) was induced by surgical 7/8 nephrectomy as previously detailed [17] and fed a high phosphorus diet (HPD: 0 .9% phosphorus, 0.6% calcium and 20% protein content) (Panlab, Barcelona, Spain) for 20 weeks. Other 10 rats were sham-operated and fed a normal phosphorus diet (NPD: 0 .6% phosphorus, 0.6% calcium and 20% protein content).

Rats were housed in wire cages and received diet and water ad libitum. The protocol was approved by the Laboratory Animal Ethics Committee of the Oviedo University. Serum creatinine, urea, albumin, calcium and phosphorus were measured at the end of study.

2.3. Experimental in vitro calcification model: primary culture of mice VSMCs overexpressing catalase

Primary cultures of VSMCs were obtained from the aorta of nephrectomized mice C57/BLJ6 wild (WT) (N= 5) and transgenic overexpressing the antioxidant enzyme catalase (Cts) (N=5) as previously described [18]. Briefly, 2- to 3- mm of aorta fragments (explants) were placed into fibronectin pre-coated (100 µg/mL) culture dishes with of Dulbecco's modified Eagle's medium (DMEM) (Lonza, Verviers, Belgium) supplemented with 20% fetal bovine serum (ThermoScientific HyClone, South Logan, UT). Pools of primary VSMC (N=5 each group) were obtained from explants of aortas from five C57/BLJ6 wild mice and five transgenic mice overexpressing catalase. Primary VSMCs were grown for four passages and cryopreserved. The cells were thawed, and the different experiments were performed between passages 6 and 8. Replicates were done with different cryopreserved cells. Cells were cultured in DMEM medium supplemented with fetal bovine serum at 10% to subconfluence and then exposed to non-calcifying medium (non-CM) with DMEM/F12 (Lonza, Verviers, Belgium) supplemented with 0.1% albumin or calcifying medium (CM) adding phosphate and calcium to non-calcifying medium reaching final concentrations of 3 and 2 mM, respectively. Cells were incubated under these conditions for 4 days. All the experiments were carried out with cells below passage 8th.

2.4. Analytical and technical procedures

2.4.1. Aortic calcification measured in kidney transplant recipient

Von Kossa staining was used to semiquantitative assessment of epigastric aortic calcifications. Tissue sections of 3 µm thickness were deparaffinised, rehydrated, and stained with an aqueous solution of 3% silver nitrate (LabKem) for 5 minutes and subsequently incubated with soda-formol solution [0.5% sodium carbonate (Merck) + 25% formaldehyde 37% (Merck)] for another 5 minutes. Sections were rinsed in 5% sodium sulphate for 5 min followed by a solution of 1% Ponceau S (Merck) + 0.5% Fuchsin Acid (Merck) for 20 minutes and then dehydrated and mounted. Calcification was assessed semi quantitatively according to staining extent: 0= negative; 1= microcalcifications; 2= mini calcifications and 3= large calcifications + a coefficient (proportion of calcified artery wall thickness + degrees of calcified artery circumference divided by 100). Patients were grouped in negative (Von Kossa score=0) and positive (von Kossa score> 0) von Kossa staining.

In addition, epigastric aortic calcification has also been measured by the o-cresolphtalein complexone method [19]. Briefly, a fragment of frozen epigastric arteria were homogenized in 0.6 N HCl at 4°C with gently shaking for 24 hours. Upon centrifugation, calcium content was determined colorimetrically in the supernatants. The remaining pellet was resuspended in lysis buffer (125 mM Tris, 2% SDS, pH 6.8) for protein extraction and quantification by DC method (Bio-Rad Laboratories). Calcium content was normalized to total cell protein and expressed as µg calcium /mg protein.

Kauppila score (KS) [20] was used to semi-quantitative assessment of abdominal aortic calcifications. Briefly, a lateral plain lumbar X-ray that included the first through fourth lumbar vertebrae was used to measure the severity of the anterior and posterior aortic calcifications on a 0-3 scale for each lumbar segment and the results were summarized in an antero-posterior severity score ranged from 0 to 24. X-ray images were evaluated by the same radiologist who was blinded to the patient's data.

2.4.2. Expression and location of catalase and RUNX2 in epigastric arteries

EnVision FLEX Mini Kit (Agilent-DAKO, K8024) and Dako Autostainer system were used for immunohistochemistry (IHC). Paraffin embedded epigastric arteries sections (3µm) were deparaffinized, rehydrated and epitope retrieval by heat induction (HIER) at 95ºC for 20 min and pH 9 (K8004, Agilent-Dako) in the Pre-Treatment Module, PT-LINK (DAKO). Endogenous peroxidase activity was blocked with EnVision™ FLEX Peroxidase-Blocking Reagent (DM821). The sections were incubated with polyclonal goat anti-catalase antibody (SC34285, 1/100; Santa Cruz Biotechnology) or polyclonal rabbit anti-RUNX2 antibody (SC10758, 1/50; Santa Cruz Biotechnology)

 doi:10.20944/preprints202307.1684.v1

and diluted in EnVision™ FLEX Antibody Diluent (Agilent-Dako K8006) for 30 minutes and afterwards with Polyclonal Rabbit Anti-Goat (P0449) for another 30 minutes only for catalase IHC. The antigen-antibody reaction was detected with the Dako EnVision + Dual Link System-HRP (Agilent-Dako) that contains goat anti-mouse and anti-rabbit immunoglobulins (Ig) conjugated to peroxidase-labelled polymer in Tris-HCl buffer. The signal was detected using diaminobenzidine chromogen as substrate in Dako EnVision™ FLEX /HRP (Agilent- Dako DM822). Sections were counterstained with hematoxylin. Negative controls were processed by omitting the primary or secondary antibody.

2.4.3. Protein analysis by 2D-DIGE

Aortas from sham-operated rats (without VC) (N=3) and nephrectomized rats fed HPD with VC (N=3) as determined by Von Kossa-positive staining [21] were pooled into 2 groups and analyzed by 2-dimensional difference gel electrophoresis (2D-DIGE). Protein identification was carried out by LC-ESI-MS/MS on a Q-TRAP instrument (Applied Biosystems, Foster City, CA) coupled to a nano-HPLC (Ultimate 3000, Dionex/LC Packings, Sunnyvale, CA). Spectra were processed with MassLynx 4.0 and database searching was done with Mascot search engine (Matrix Science) against UniProt release 2011_11 as previously described [16]. A protein was considered identified when at least two different peptides were detected. Protein localization and function was assigned according to PubMed and SwissProt information.

2.4.4. Catalase protein levels and activity in VSMCs primary culture

For Western-blot, total proteins from WT and Cts were collected in RIPA buffer and quantified by Bradford assay (Bio-Rad). Equal amounts of protein (30 µg) were subjected to electrophoresis and transferred to PVDF using SDS-PAGE following standard procedures. After 1 hour incubation in 3% BSA-TRIS blocking solution, protein detection was performed using specific antibodies for catalase (sc-34285) and beta-actin (MS-1295-P, Neomarkers). Membranes were incubated overnight at 4 ºC at 1:5000 dilution and 1:8000 dilution respectively. Secondary antibodies were incubated for 1 hour at room temperature (1:10000 dilution rabbit antigoat IgG for catalase, Cat: 401504, Calbiochem; 1:10000 dilution goat anti-mouse IgG for beta-actin, Cat: 401215, Calbiochem). Chemiluminescence was digitized and quantified with ChemiDoc™ XRS+ instrument (Bio-Rad, Hercules, CA) and the ImageLab™ software. Densitometric values of catalase are shown as a ratio of the correspondent actin values on the same line.

The basal activity of catalase was measured in VSMC from WT and Cts using the commercial kit "catalase assay kit" (Cayman Chemical), following the protocol established by the manufacturer.

2.4.5. RUNX2 in VSMCs primary culture

Cells from mice, both WT and Cts cultured with non-CM and CM, were fixed with methanol: ethanol (1:1) for 10 min and treated with 0.1% Tween 20 + 5% bovine serum albumin (BSA) for 1h at room temperature. Then, cells were incubated with a rabbit anti-RUNX2 polyclonal antibody (1:50 dilution; sc-10758, Santa Cruz Biotechnology) overnight at 4ºC followed by anti-rabbit Alexa Fluor 594 (1:400 dilution; A21207, Cell Signaling Technology). Cells were counterstained with 4',6-diamidino-2-phenylindole (DAPI) added to mounting medium (SlowFade™ Diamond Antifade Mountant with DAPI, ThermoFisher).

2.4.6. Quantification of calcium content in VSMCs primary culture

VSMCs cultured with non-CM and CM were washed with PBS and homogenized in 0.6 N HCl and calcium content was determined by the o-cresolphtalein complexone method described in point 2.4.1.

Preprints (www.preprints.org) | NOT PEER-REVIEWED | Posted: 26 July 2023 doi:10.20944/preprints202307.1684.v1

2.4.7. Redox metabolism probes in VSMCs primary culture

Redox state was assessed in the cytoplasm and in the mitochondria, Dichlorofluorescein-di-acetate (DCF, Invitrogen) and Di-hydro-rhodamine 123 (DHR123, Invitrogen) respectively were used. VSMC incubated with calcium and phosphorus or in control conditions (see 2.3) were washed with Hank´s solution and then incubated for 30 min. (darkness, 36 º and 5% CO_2) in a Hank's solution with both 500 nM DCF- and 10 μM DHR123. Five confluent fields of each experimental replicates were acquired first for DCF and then for DHR123, alternating non-CM and CM conditions in order to minimize bias.

2.5. Imaging analyses

Images of epigastric arteries were acquired under a light microscope (DMRXA2, Leica Microsystems). In VSMCs analysis, fluorescent images were acquired using Nikon Eclipse TS100 microscope.

2.5.1. Catalase in epigastric arteries

Whole slides were scanned in a Hammamatsu NanoZoomer (20x magnification) and images were analysed by using QPath (v 0.3.2). Images were defined as Brightfield-HDAB. Non-calcification area and peri-calcification ROIs in media layer were selected manually by using wand tool. A pixel classifier was applied to ROIs (Threshold DAB channel 0.14 at Low (7.06 μm/px) resolution). Percentage of catalase positive staining area was obtained.

2.5.2. RUNX2 in epigastric arteries

The ratio between positive nuclei for RUNX2 and the total number of nuclei were calculated in each whole epigastric artery section (20x magnification). For total protein levels, Fiji software was used, images were deconvoluted following H-DAB vector. A threshold at 171 was applied to the image corresponding to DAB channel. Media layer surface ROI was draw in the original image and applied to the DAB channel for positive area measurement.

For peri-calcification area, in the images where a calcification was observed, the proportion of media layer covering the length of the calcification was considered peri-calcification area. Non-calcification area was quantified in the same image when a safe margin of 50 microns was between the lesion and the non-calcified area. Positive area quantification was performed as described for total protein levels. For nuclear quantification, the Hematoxilin channel from the H-DAB deconvolution (marking nuclei) was used as ROI mask in DAB channel, obtaining the positive DAB areas in nuclear ROI only.

2.5.3. RUNX2 in VSMCs primary culture

Micrographs were analysed using FIJI software [22]. For total Runx2 levels, all the images were corrected (brightness and contrast) at 36-168. For total fluorescence intensity, total cell contour was delimitated as a single ROI and average fluorescence intensity was measured. Quantification of nuclear RUNX2 staining area was generated using a nuclear ROI from the DAPI staining (blue channel). The RUNX2 images were converted to black and white, a threshold of 16 was applied to the images. Positive pixel area of RUNX2 was quantified in the DAPI-based ROI only.

2.5.4. Redox metabolism probes in VSMCs primary culture

Micrographs were analyzed using FIJI software. The protocol was analogous to the one described in point 2.5.3. Total DCF and DHR123 levels were measured. No correction was applied. Total field was quantified.

Preprints (www.preprints.org) | NOT PEER-REVIEWED | Posted: 26 July 2023 doi:10.20944/preprints202307.1684.v1

2.6. Statistical analysis

For statistical analysis and graphs Prism GraphPad (v 9.2.0) was used. All experimental groups were tested for normality by using Shapiro-Wilk test and Kolmogorov-Smirnov, when one or both of these tests were positive for all experimental groups, samples were considered to follow a normal distribution and analyzed by t-test (paired or unpaired in each case). One or more experimental groups were not following a normal distribution Kolmogorov-Smirnov for cumulative distributions or Wilcoxon matched pairs test were used. All values are shown as mean ± SD unless otherwise is indicated.

3. Results

3.1. Catalase and RUNX2 protein levels in epigastric arteries of kidney transplant recipients

This study included 17 epigastric arteries from kidney transplant recipients. The main characteristics of patients are summarized in Table 1. Epigastric arteries were classified as calcified or non-calcified on the basis of von Kossa staining (Supplementary Figure 1A). There was no difference either in age, sex, smoke habit, body mass index (BMI), arterial hypertension, hyperlipidaemia, time on dialysis, serum phosphate and calcium levels among groups. Kauppila score and epigastric calcium content showed significant association with von Kossa grouping, supporting the methodology chosen for the staging.

Table 1. Patient characteristics classified according to von Kossa staining:.

	Von Kossa Staining		
	Negative	**Positive**	**p-value**
n	**7**	**10**	
Sex = Male (%)	7 (100.0)	9 (90.0)	1.000
Age (years) (mean (SD))	60.6 (7.9)	57.5 (7.0)	0.412
Smoking habit = Yes (%)	1 (14.3)	2 (20.0)	1.000
BMI (kg/m2) (mean (SD))	26.8 (5.0)	25.4 (5.4)	0.588
Hypertension = Yes (%)	7 (100.0)	9 (90.0)	1.000
Hyperlipidaemia = Yes (%)	4 (57.1)	5 (50.0)	1.000
Time on dialysis (months) (mean (SD))	17.1 (12.5)	30.3 (14.2)	0.068
Serum phosphate (mg/dl) (mean (SD))	4.2 (1.2)	4.2 (1.1)	0.999
Serum calcium (mg/dl) (mean (SD))	9.1 (0.8)	8.6 (0.5)	0.147
Kauppila score (mean (SD))	2.3 (2.8)	9.0 (6.0)	0.015
Von Kossa score (mean (SD))	0.0 (0.0)	3.9 (2.4)	0.001
Calcium content (ug/mg protein) (mean (SD))	15.3 (2.1)	957.2 (993.1)	0.038
Catalase protein levels (A.U.) (mean (SD))	11.2 (6.6)	9.5 (11.3)	0.738
RUNX2 protein levels (A.U.) (mean (SD))	0.9 (0.1)	0.7 (0.2)	0.062
RUNX2 positive nuclei/Total nuclei (mean (SD))	0.1 (0.1)	0.2 (0.2)	0.681

SD: Standard deviation; BMI: Body mass index; A.U.: Arbitrary units.

As we previously mentioned, previous studies found *in vitro* a protective effect of catalase in vascular calcification induced by calcium and phosphorous [14]. Low levels of catalase would help to explain why some CKD patients develop vascular calcification. To confirm the relevance of these findings, the catalase protein levels in the media layer of the epigastric arteries from kidney transplant recipients were analysed using IHC. The results did not show a relationship between catalase levels in the arteries and patient's von Kossa staining calcium content or Kauppila score (Table 1).

When possible, the levels of catalase surrounding the calcification, were also analysed. Interestingly, when we compared the average levels of catalase in the media layer of the area surrounding the calcified tissue, catalase was significantly increased in peri-calcified areas (Figure 1A and B). This increase was localized in specific areas; therefore, it might be circumscribed to

Preprints (www.preprints.org) | NOT PEER-REVIEWED | Posted: 26 July 2023 doi:10.20944/preprints202307.1684.v1

individual cells (arrow heads). This result indicates a dual expression of catalase within the same tissue depending on the calcification intensity of the area.

Additionally, RUNX2 levels were also analysed in these sections (Table 1). There was not a significant increase of RUNX2 in either calcified and non-calcified groups either total or nuclear. When the protein levels of RUNX2 were studied in peri-calcification areas, no changes in total protein were observed. However, nuclear RUNX2 staining showed a decreasing trend in the peri-calcification areas (p-value= 0.062) (Figure 1C, D and Supplementary Figure 1B). The results showed that, in peri-calcification areas, where catalase levels were higher, RUNX2 levels did not change but they tend to have a cytoplasmic rather than nuclear staining.

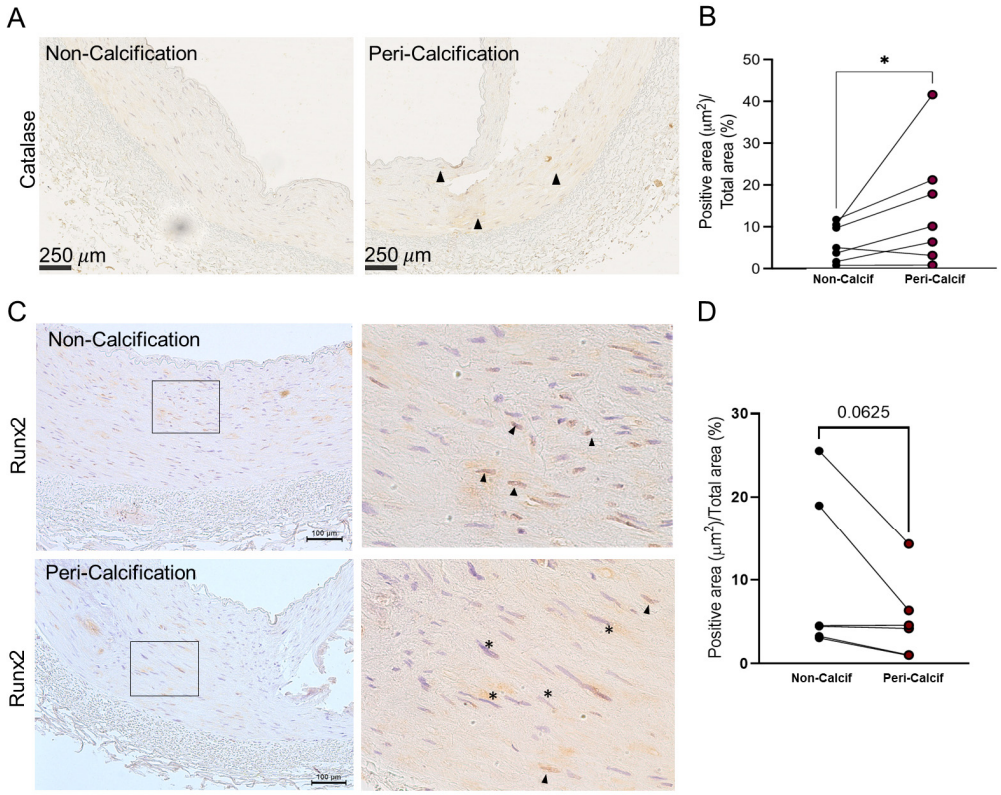

Figure 1. Catalase and RUNX2 protein levels in epigastric arteria of kidney transplant recipients. A) Catalase immunostaining of non-calcification and peri-calcification areas of the same epigastric arteria section (arrow heads shows localized staining). B) Catalase positive immunostaining quantification for non-calcification and peri-calcification areas. C) RUNX2 immunostaining of non-calcification and peri-calcification areas of the same epigastric arteria section. Right, zoomed areas indicated on left images (square) showing nuclear Runx2 staining, positive black arrow heads, negative (*). D) RUNX2 positive immunostaining quantification for non-calcification and peri-calcification areas. All panels Mean±SD, for D) and H) *=p-value<0.05 Wilcoxon paired test. Peri-Calcif. means peri-calcified area; Non-Calcif. means non-calcification area.

3.2. Differential protein expression in aortas from rats with and without VC

To characterize general features of VC-CKD, we studied a rat animal model of VC induced by CRF and a HPD (see materials and methods).

Rats with VC showed impairment of renal function and mineral metabolism as measured by higher serum creatinine, urea, P, lower serum albumin and no changes in serum calcium compared to rats without VC (No-VC) (Supplementary Table 1).

Proteomic analysis was performed in aortas. 2D-DIGE analysis detected approximately 3400 protein spots of which 77 were differentially expressed in calcified and non-calcified aortas. At least 2 peptides were identified in 26 of the 77 proteins differentially expressed; 5 of them direct or

Preprints (www.preprints.org) | NOT PEER-REVIEWED | Posted: 26 July 2023 doi:10.20944/preprints202307.1684.v1

indirectly related to oxidative stress (Table 2). From those 5, 3 were directly related with mitochondrial redox metabolism: superoxide dismutase (SODM), GSH peroxidase 3 (GPX3) and glutathione-S-transferase type Mu2 (GSTM2). In calcified aorta there was an increase (2.14-fold change) in mitochondrial superoxide dismutase (SODM) compared to non-calcified ones. The metabolism of the main antioxidant glutathione is another main difference between calcified and non-calcified samples. There was a significant decrease of GPX3 in calcified aortas, which has an analogous role to catalase scavenging extracellular H_2O_2. GSTM2, also decreased in calcified tissue, takes part in xenobiotic metabolism and detoxification.

Table 2. Differential protein expression pattern in calcified compared with non-calcified aortas showed as average ratio. Protein spots differentially expressed shown in Figure 2 were identified by LC-MS/MS (Supplementary Table 2 and supplementary annexe).

Spot Nº	MASCOT -Symbol	Name	Accession Nº	Function	Localization	T-test p value	Average Ratio	Score	MW (Da)	pI	Number of peptides identified
1	CAH3	Carbonic anhidrase 3	P14141	Carbonate dehydratase activity	Cytoplasm	0.0042	4.86	95	29413	6.89	3
2	GPX3	Glutathione peroxidase 3	P23764	Protects cells and enzymes from oxidative damage, by catalyzing the reduction of hydrogen peroxide, lipid peroxides and organic hydroperoxide, by glutathione.	Extracellular space	0.0052	-2.76	97	25637	8.26	2
3	GSTM2	Glutathione S-transferase Mu2	P08010	Conjugation of reduced glutathione to a wide number of exogenous and endogenous hydrophobic electrophiles. Participates in the formation of novel hepoxilin regioisomers	Cytoplasm	0.0018	-2.38	234	25857	6.9	7
4	SODM	Superoxide dismutase [Mn], mitochondrial precursor	P07895	Destroys superoxide anion radicals which are normally produced within the cells and which are toxic to biological systems	Mitochondrion matrix	0.0087	2.14	113	24887	8.96	2

Preprints (www.preprints.org) | NOT PEER-REVIEWED | Posted: 26 July 2023 doi:10.20944/preprints202307.1684.v1

5	TKT	Transketolase	P50137	Catalyzes the transfer of a two-carbon ketol group from a ketose donor to an aldose acceptor, via a covalent intermediate with the cofactor thiamine pyrophosphate.	Intracellular membrane	0.0041	-1.62	43	68342	7.23	2

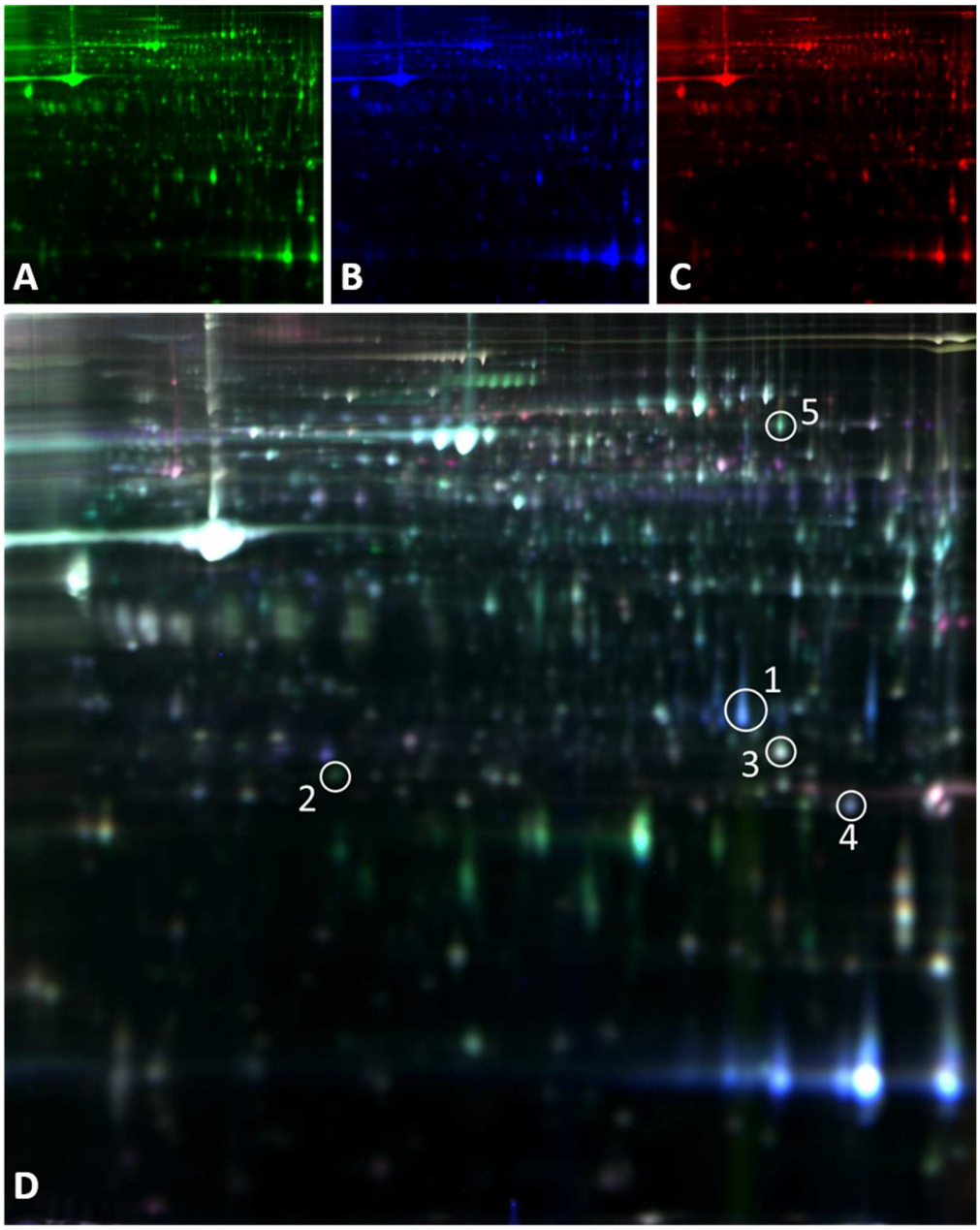

Preprints (www.preprints.org) | NOT PEER-REVIEWED | Posted: 26 July 2023 doi:10.20944/preprints202307.1684.v1

Figure 2. 2D-DIGE images showing proteins differentially expressed between calcified and non-calcified aortas. A) Cy5-labeled proteins from non-calcified aortas; B) Cy2- labelled proteins from calcified aortas; C) Cy3 dye staining of the internal standard and D) The merging of A, B and C. Circled spots are those proteins differentially expressed that were direct or indirectly related to oxidative stress listed in Table 2.

3.3. In vitro model of vascular calcification in VSCMs overexpressing catalase.

Primary cell culture of VSMCs was obtained from WT and transgenic mice for Cts overexpression. VMSC exhibited 12 times fold increase of Cts protein levels and a concomitant increase in Cts activity (Supplementary Figure 2A and B), similar results were reported elsewhere [14].

When incubated with CM, WT and Cts VSMCs showed a significant increase in calcium content although the differences were less pronounced in Cts group (Figure 3B).

Cts VSMCs showed significantly higher levels of RUNX2 compared with WT cells under non-CM conditions. RUNX2 expression was also significantly increased in both WT and Cts after exposure to CM (Figure 3A and C). However, the percentage of the nucleus stained for RUNX2 was significantly higher in WT cells cultured with CM compared WT cells cultured with non-CM (Figure 3A and D) this increase was not observed in Cts-CM. Negative controls for rabbit anti-RUNX2 primary and anti-rabbit Alexa Fluor 594 secondary antibody are shown (Supplementary Figure 3).

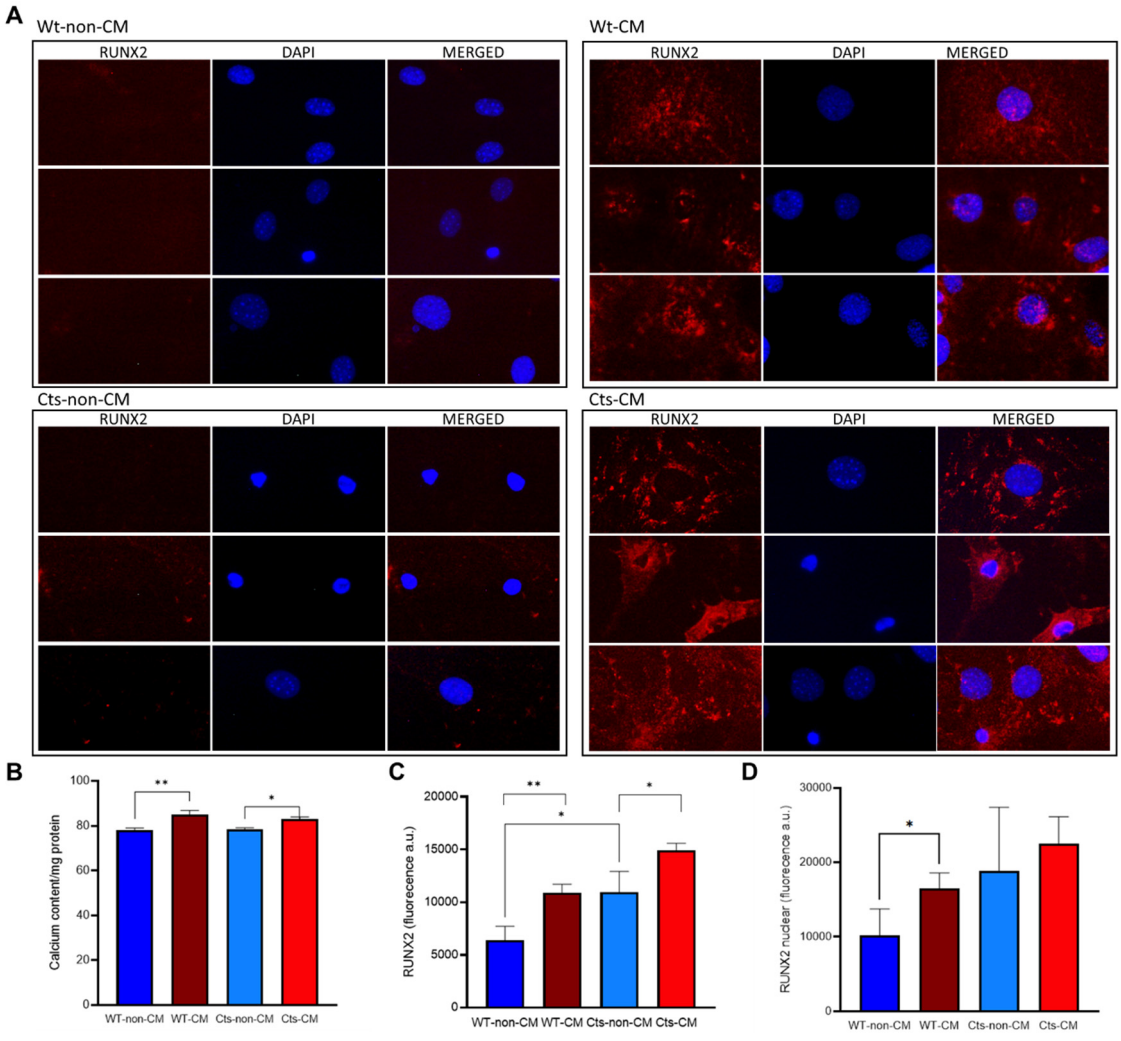

Figure 3. VSMC primary culture from WT and catalase (Cts) overexpressing mice incubated with high CM. A) Immunocytochemistry of Runx2 (red) in WT and Cts VSMC exposed to non-CM and

Preprints (www.preprints.org) | NOT PEER-REVIEWED | Posted: 26 July 2023 doi:10.20944/preprints202307.1684.v1

CM, DAPI (blue) is used as nuclear counter-staining. B) Calcium content in non-CM and CM of WT and Cts VSMCs. C) Total Runx2 fluorescence quantification. D) nuclear Runx2 fluorescence quantification. All panels Mean±SD, B), D) and E) *=p-value<0.05, **=p-value<0.01. B), C) and D) Unpaired t-test.

Basal cytoplasmic redox state, as measured by DFC average fluorescence intensity and positive area, was higher in Cts cells compared with WT cells (Figure 4A, B and C). Fluorescence intensity was greater in WT cells cultured with CM compared with non-CM without differences in the fluorescence area. Noteworthy, the increase found in the fluorescence intensity is based on a subset of cells which drastically increased their fluorescence while the majority of the culture did not show changes in the redox state (Figure 4A). Cts cells showed no differences between CM and non-CM in both, fluorescence intensity and fluorescent area (Figure 4B and C).

No relevant changes were observed in mitochondrial redox state, measured by DHR123 fluorescence intensity, either in WT or Cts VSMCs at non-CM or CM conditions (Figure 4 A, D and E).

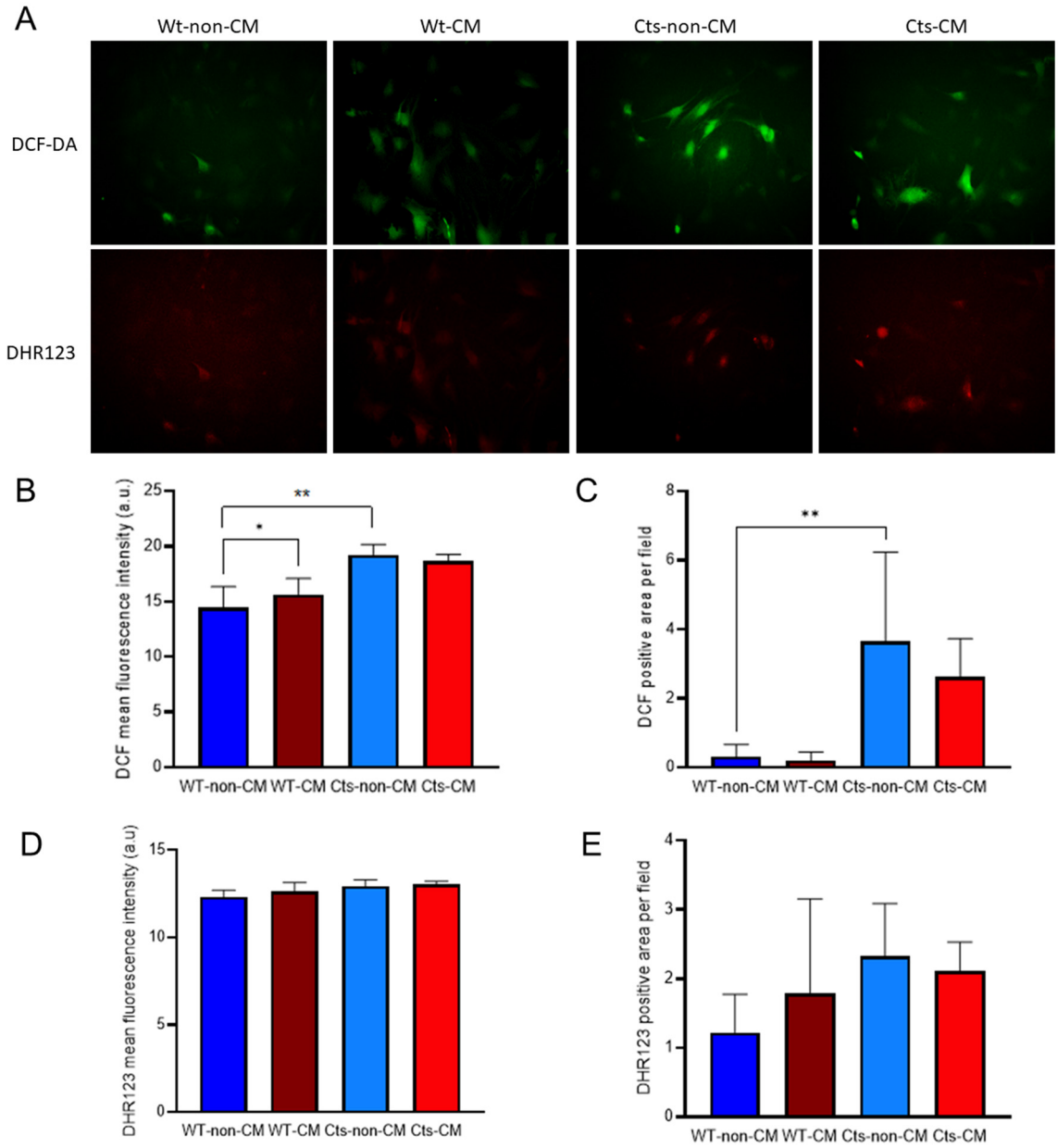

 doi:10.20944/preprints202307.1684.v1

Figure 4. Redox state in VSMC primary culture from WT and catalase (Cts) overexpressing mice incubated with non-CM and CM. A) Micrographies of cytoplasmic redox state monitored with DCF-DA and DHR123 in VSMC cultured with non-CM and CM. B) DCF-DA average fluorescence intensity. C) DCF-DA positive area (px). D) DHR123 average fluorescence intensity. E) DCF-DA positive area(px). All panels Mean±SD, B) and C) *=p-value<0.05, **=p-value<0.01. Kolmogorov-Smirnov test.

4. Discussion

VC was considered as a passive deposit of hydroxyapatite crystals, however, this simplistic theory was discarded two decades ago to open a much more complex scenario. Similarly oxidative stress theory in the context of VC was considered as a black or white factor. The increase of free radicals has been associated with VC meanwhile the absence or low levels has been associated to a low incidence of VC. However, similarly to what it has been observed in other biological scenarios these explanations might be an oversimplification of the role of oxidative stress and redox metabolism.

In the present work the epigastric arteries from CKD patients undergoing kidney transplant showed a moderate and local increase of catalase, one of the main H_2O_2 scavengers, surrounding the calcification which coexisted with a trend towards total RUNX2 expression without increase in nuclear RUNX2 stain in the same surrounding areas. These peri-calcification areas probably show a heterogeneous territory, with cells that could be trying to protect themselves from calcification process, with less degree of calcification as the main areas of VC were lost during the tissue processing.

Among proteins differentially expressed in calcified and non-calcified aortas in an animal model of VC, deregulation of several proteins related with oxidative stress were observed. Catalase was not identified, but a decrease of an analogous as GPX3 in calcified aortas was found. The decreases levels of extracellular H_2O_2 scavenges found in the aortas, would be related to the severe VC found. It is important to highlight that these results are referred to protein levels, therefore a further confirmation of these changes at enzymatic activity level would be ideal. However, the limited amount of sample, particularly in the human studies, made not possible further analyses.

To better understand the role of catalase, an *in vitro* model was used. An increase of calcium deposits and RUNX2 at total protein and nuclear levels in VSMC in WT cells in the CM was found. However, when catalase was overexpressed and cultured with CM, there was a mild increase in calcium content without a significant concomitant increase in nuclear RUNX2 stain. This decrease of nuclear RUNX2 stain could partially prevent VC onset and this result is consistent with those found in the epigastric arteries from CKD patients. A relevant finding was the fact that calcium content and RUNX2 total protein levels increased when catalase was overexpressed in VSMC cultured in non-CM conditions, suggesting that catalase might affect calcium metabolism directly (Supplementary Figure 2C).

This might not be just a coincidence as H_2O_2 is able to affect calcium release of the main intracellular calcium storages, mitochondria and endoplasmic reticulum, increase calcium release from both storage organelles and uptake from the extracellular space increasing calcium cytoplasmic content [23]. Therefore, regulation of antioxidant enzymes specialized on H_2O_2 elimination such as catalase or GPX3, as it has been, would allow to keep similar amounts of intracellular calcium but confined to calcium storages. In the specific case of GPX3 (extracellular form), it could also inhibit the calcium uptake from the extracellular space. A fine-tuned range of catalase or peroxidase concentration would allow the cells to control intracellular calcium levels keeping cell stiffness in contractile phenotype [24]. The present results show that catalase could be able of reduce VC at early stages even in the presence of increased calcium levels and RUNX2 expression.

This counterbalance effect is not permanent and upon a long-term calcification stimulus the peri-calcification areas observed in the epigastric arteries may calcified completely. In fact, the *in vivo* model of severe VC showed that antioxidant actions were not observed and the expression of GPX3

and GST were decreased. In the same line, oxidative stress as inductor of VSMCs to osteoblast differentiation has been shown by other authors [25,26].

Even though there is no correlation between total catalase and Von Kossa staining (p-value: 0.097) nor with KS (p-value: 0.6778), our study reflects a local increase of catalase surrounding the calcification lesion and this increase has been observed in specific cells. This increase was not expected as previous reports described only an increase of catalase in the calcification lesions [27]. To interpret our results two arguments can be considered, the first is the above mentioned description was made on an *in vivo* model of aortic valve calcification without renal damage. In this model although there was free radical production, the oxidative stimuli seems to be from mitochondrial origin, while by contrast, in VC associated to CKD the stimuli has a very strong cytoplasmic origin caused by NOX enzymatic system [4,28]. The second is that our *in vitro* model showed that the overexpression of catalase is confined at the peroxisome organelle, and it does not necessarily cause a decrease in cytoplasmic redox state.

Upon superoxide radical production at NOX enzymatic system, catalase would need from the CuZnSOD to convert superoxide on H_2O_2 a non-charged molecule that would be able to pass the peroxisome membrane to reach the catalase. This might be important in the case of VSMCs where NOX enzyme are constitutively expressed as they have a role in vesicle trafficking and muscle contraction [29]. The excess of superoxide might favour the reaction with other radical groups forming such as NO or Fe^{3+}-H_2O forming peroxynitrate or hydroxyl radical which will also produce DCF-DA fluorescence.

A previous study showed that catalase overexpression prevented both, calcium deposition and the increase of RUNX2 levels in VSMCs cultured with CM for 8 days [14], however, the mechanisms by which catalase was able to prevent calcification was not detailed. The present study allowed us to study the calcification process at earlier stages, 4 days of culture, before the calcification occurred. In the early stage of the calcification process (only 8% increase in calcium content), no differences were observed in mitochondrial oxidative stress levels compared in WT. The total RUNX2 levels increased in both WT and Cts cells cultured with CM, also, as we mentioned above RUNX2 levels were also increased in Cts non-CM. However, nuclear RUNX2 did not increase significantly in the Cts cells cultured with CM.

These results suggest that catalase overexpression may block the translocation of RUNX2 to the nucleus and thus the trans-differentiation from VSMCS to osteoblast-like cells. Nevertheless, images obtained with a conventional fluorescence microscopy only analyzed in a 2D plane and have some limitations to study nuclear localization. Then, further studies using confocal microscopy are needed to corroborate nuclear RUNX2 localization under these conditions. Our hypothesis is that at this early stage, both cell lines respond to CM stimuli but catalase delays VC by abolishing RUNX2 nuclear translocation. However, it is very unlikely that these levels can be observed in non-manipulated tissues, therefore if the calcification stimuli persist, the antioxidant response (catalase, peroxidase) would fail and the calcification would occur.

The clinical significance derived from the results of the present study is that antioxi-dants may have beneficial effects in delaying osteogenic transdifferentiation of vascular smooth muscle cells and thus vascular calcification. Although, the particularities of the catalase-calcium relationship in the context of the muscular media layer present a very complex scenario beyond the mere antioxidant scavenging enzyme. This complexity would allow to understand the results obtained in previous studies investigating the likely protective role of catalase in CKD and in vascular diseases [12,13], where no positive results were obtained, despite catalase is the most efficient H_2O_2 vascular scavenger and having CKD and VC a very strong oxidative stress component.

Supplementary Materials: The following supporting information can be downloaded at the website of this paper posted on Preprints.org. Supplementary Figure 1: Representative images of von Kossa staining. A) Epigastric arteria negative and positive for von kossa staining. B) Micrographies of distant and peri-calcification areas of the same epigastric arteria section for von Kossa staining. Supplementary Figure 2: VSMCs from Wild-type (WT) and Catalase (Cts) cell culture. A) Western-Blot for catalase protein expression, representative image of western-blot (upper panel), quantification of optical density (lower panel). B) Cts activity in VSMC cell culture. C) Calcium content per mg of protein in WT cell culture and Cts overexpressing cells. Each pair correspond to

one individual experiment. Supplementary Figure 3. Immunofluorescence of RUNX2 in VSMCs. Negative controls for primary (rabbit anti-RUNX2) and secondary antibody (anti-rabbit Alexa Fluor 594). DAPI is used as nuclear counter-staining. Supplementary Table 1: Biochemical parameters of sham- operated rats with normal renal function without vascular calcification (No-VC) and nephrectomised rats fed a high phosphorus diet (HPD) with vascular calcification (VC) at 20 weeks. Supplementary Table 2. Summary of the peptides identified by LC-MS/MS.

Author Contributions: Conceptualization, I.Q.G., C.A.M, N.C.L., S.P.G., J.L.F.M., J.B.C.A, J.C.M.B. and M.N.D.; methodology, I.Q.G, C.A.M., N.C.L., S.P.G, B.M.C., P.R.G., R.G.C., J.M.F.G., M.A.H.S., J.M.V., S.F.V., L.M.A., S.B.V. and L.C.B.; formal analysis, I.Q.G, J.L.F.M., N.C.L., S.P.G., J.B.C.A., M.N.D. and C.A.M; investigation, I.Q.G; C.A.M. and S.B.V.; resources, J.L.F.M., C.A.M., N.C.L., S.P.G. and M.N.D; writing—original draft preparation, I.Q.G. and C.A.M.; writing—review and editing, J.L.F.M., N.C.L., S.P.G., J.B.C.A. and M.N.D ; visualization, I.Q.G, J.L.M.F. and C.A.M ; supervision, J.C.M.B., J.B.C.A., M.N.D, and J.L.F.M.; project administration, C.A.M., J.L.F.M; J.B.C.A. and I.Q.G.; funding acquisition, C.A.M, J.L.F.M., S.P.G., N.C.L., M.N.D., J.B.C.A.; All authors have read and agreed to the published version of the manuscript.

Funding: This study has been funded by Instituto de Salud Carlos III (ISCIII) through the project RD12/0021/0023 and RD16/0009/0017, and RD21/0005/0019 and by Next Generation EU; Recovery, Transformation and Resilience Plan, and through the project PI11-00667, PI14/00707, PI17/00384 and PI20/00633 (co-funded by the European Union), Plan Estatal de I+D+I 2013-2016 , Plan de Ciencia, Tecnología e Innovación 2013-2017 y 2018-2022 del Principado de Asturias (GRUPIN14-028, IDI-2018-000152, IDI/2021/000080).

Institutional Review Board Statement: The study in humans was conducted in accordance with the Declaration of Helsinki and approved by the Research Ethics Committee of the Principality of Asturias (code 42/2011 approved on 28/04/2011). The animal study protocol was approved by the (PROAE 14-2021 approved on 05/05/20521) and Laboratory Animal Ethics Committee of the Alcalá University (CEI 2012/028/01/20120322 approved on 12/04/2012).

Informed Consent Statement: Informed consent was obtained from all subjects involved in the study.

Data Availability Statement: The data presented in this study are available on request from the corresponding authors.

Acknowledgments: We acknowledge Francisco Otero García and Pilar Alonso Suarez from the Transplant Coordination Unit of the Hospital Universitario Central de Asturias for their help in the collection and BioBanco del Pincipado de Asturias for their help in the processing, custody and immunohistochemistry of epigastric arteries. We also thank to ALCER (Asociación para la lucha contra las enfermedades renales de Asturias) for their support to basic research.

Conflicts of Interest The authors declare no conflict of interest.

References

1. Román-García, P.; Rodríguez-García, M.; Cabezas-Rodríguez, I.; López-Ongil, S.; Díaz-López, B.; Cannata-Andía, J.B. Vascular Calcification in Patients with Chronic Kidney Disease: Types, Clinical Impact and Pathogenesis. *Med. Princ. Pract.* **2011**, *20*, 203–212, doi:10.1159/000323434.
2. Levey, A.S.; Eckardt, K.U.; Tsukamoto, Y.; Levin, A.; Coresh, J.; Rossert, J.; De Zeeuw, D.; Hostetter, T.H.; Lameire, N.; Eknoyan, G.; et al. Definition and Classification of Chronic Kidney Disease: A Position Statement from Kidney Disease: Improving Global Outcomes (KDIGO)Z. *Kidney Int.* **2005**, *67*, 2089–2100, doi:10.1111/j.1523-1755.2005.00365.x.
3. Nelson, A.J.; Raggi, P.; Wolf, M.; Gold, A.M.; Chertow, G.M.; Roe, M.T. Targeting Vascular Calcification in Chronic Kidney Disease. *JACC Basic to Transl. Sci.* **2020**, *5*, 398–412, doi:10.1016/j.jacbts.2020.02.002.
4. Tóth, A.; Balogh, E.; Jeney, V. Regulation of Vascular Calcification by Reactive Oxygen Species. *Antioxidants* **2020**, *9*, 1–24, doi:10.3390/antiox9100963.
5. Kramer, H.; Toto, R.; Peshock, R.; Cooper, R.; Victor, R. Association between Chronic Kidney Disease and Coronary Artery Calcification: The Dallas Heart Study. *J. Am. Soc. Nephrol.* **2005**, *16*, 507–513, doi:10.1681/ASN.2004070610.
6. Sies, H.; Jones, D.P. Reactive Oxygen Species (ROS) as Pleiotropic Physiological Signalling Agents. *Nat. Rev. Mol. Cell Biol.* **2020**, *21*, 363–383, doi:10.1038/s41580-020-0230-3.
7. Kraehling, J.R.; Sessa, W.C. Contemporary Approaches to Modulating the Nitric Oxide-CGMP Pathway in Cardiovascular Disease. *Circ. Res.* **2017**, *120*, 1174–1182, doi:10.1161/CIRCRESAHA.117.303776.
8. Byon, C.H.; Heath, J.M.; Chen, Y. Redox Signaling in Cardiovascular Pathophysiology: A Focus on Hydrogen Peroxide and Vascular Smooth Muscle Cells. *Redox Biol.* **2016**, *9*, 244–253,

doi:10.1016/j.redox.2016.08.015.

9. Chang, H.B.; Javed, A.; Dai, Q.; Kappes, J.C.; Clemens, T.L.; Darley-Usmar, V.M.; McDonald, J.M.; Chen, Y. Oxidative Stress Induces Vascular Calcification through Modulation of the Osteogenic Transcription Factor Runx2 by AKT Signaling. *J. Biol. Chem.* **2008**, *283*, 15319–15327, doi:10.1074/jbc.M800021200.
10. Roman-Garcia, P.; Barrio-Vazquez, S.; Fernández-Martín, J.L.; Ruiz-Torres, M.P.; Cannata-Andia, J.B. Natural Antioxidants and Vascular Calcification: A Possible Benefit? *J. Nephrol.* **2011**, *24*, 669–672, doi:10.5301/jn.5000029.
11. Nivet-Antoine, V.; Labat, C.; El Shamieh, S.; Dulcire, X.; Cottart, C.H.; Beaudeux, J.L.; Zannad, F.; Visvikis-Siest, S.; Benetos, A. Relationship between Catalase Haplotype and Arterial Aging. *Atherosclerosis* **2013**, *227*, 100–105, doi:10.1016/j.atherosclerosis.2012.12.015.
12. Crawford, A.; Fassett, R.G.; Coombes, J.S.; Kunde, D.A.; Ahuja, K.D.K.; Robertson, I.K.; Ball, M.J.; Geraghty, D.P. Glutathione Peroxidase, Superoxide Dismutase and Catalase Genotypes and Activities and the Progression of Chronic Kidney Disease. *Nephrol. Dial. Transplant.* **2011**, *26*, 2806–2813, doi:10.1093/ndt/gfq828.
13. Hishida, A.; Okada, R.; Naito, M.; Morita, E.; Wakai, K.; Hamajima, N.; Hosono, S.; Nanri, H.; Turin, T.C.; Suzuki, S.; et al. Polymorphisms in Genes Encoding Antioxidant Enzymes (SOD2, CAT, GPx, TXNRD, SEPP1, SEP15 and SELS) and Risk of Chronic Kidney Disease in Japanese - Cross-Sectional Data from the J-MICC Study. *J. Clin. Biochem. Nutr.* **2013**, *53*, 15–20, doi:10.3164/jcbn.13-17.
14. Martínez Arias, L.; Panizo García, S.; Carrillo López, N.; Barrio Vázquez, S.; Quirós González, I.; Román García, P.; Mora Valenciano, I.; Miguel Fernández, D.; Añón álvarez, E.; Fernández Martín, J.L.; et al. Effects of the Catalase Antioxidant Enzyme in Vascular Calcification and Bone Demineralization. *Rev. Osteoporos. y Metab. Miner.* **2017**, *9*, 13–19, doi:10.4321/S1889-836X2017000100003.
15. Román-García, P.; Carrillo-López, N.; Fernández-Martín, J.L.; Naves-Díaz, M.; Ruiz-Torres, M.P.; Cannata-Andía, J.B. High Phosphorus Diet Induces Vascular Calcification, a Related Decrease in Bone Mass and Changes in the Aortic Gene Expression. *Bone* **2010**, *46*, 121–128, doi:10.1016/j.bone.2009.09.006.
16. Quirós-González, I.; Román-García, P.; Alonso-Montes, C.; Barrio-Vázquez, S.; Carrillo-López, N.; Naves-Díaz, M.; Mora, M.I.; Corrales, F.J.; López-Hernández, F.J.; Ruiz-Torres, M.P.; et al. Lamin A Is Involved in the Development of Vascular Calcification Induced by Chronic Kidney Failure and Phosphorus Load. *Bone* **2016**, *84*, 160–168, doi:10.1016/j.bone.2016.01.005.
17. Naves-Díaz, M.; Carrillo-López, N.; Rodríguez-Rodríguez, A.; Braga, S.; Fernández-Coto, T.; Lopez-Novoa, J.M.; López-Hernández, F.; Cannata-Andía, J.B. Differential Effects of 17β-Estradiol and Raloxifene on Bone and Lipid Metabolism in Rats with Chronic Kidney Disease and Estrogen Insufficiency. *Menopause* **2010**, *17*, 766–771, doi:10.1097/gme.0b013e3181ce6874.
18. Martínez Arias, L.; Panizo García, S.; Carrillo López, N.; Barrio Vázquez, S.; Quirós González, I.; Román García, P.; Mora Valenciano, I.; Miguel Fernández, D.; Añón álvarez, E.; Fernández-Martín, J.L.; et al. Effects of the Catalase Antioxidant Enzyme in Vascular Calcification and Bone Demineralization. *Rev. Osteoporos. y Metab. Miner.* **2017**, *9*, 13–19, doi:10.4321/S1889-836X2017000100003.
19. Carrillo-López, N.; Panizo, S.; Alonso-Montes, C.; Martínez-Arias, L.; Avello, N.; Sosa, P.; Dusso, A.S.; Cannata-Andía, J.B.; Naves-Díaz, M. High-Serum Phosphate and Parathyroid Hormone Distinctly Regulate Bone Loss and Vascular Calcification in Experimental Chronic Kidney Disease. *Nephrol. Dial. Transplant.* **2019**, *34*, 934–941, doi:10.1093/ndt/gfy287.
20. Kauppila, L.I.; Polak, J.F.; Cupples, L.A.; Hannan, M.T.; Kiel, D.P.; Wilson, P.W.F. New Indices to Classify Location, Severity and Progression of Calcific Lesions in the Abdominal Aorta: A 25-Year Follow-up Study. *Atherosclerosis* **1997**, *132*, 245–250, doi:10.1016/S0021-9150(97)00106-8.
21. Gómez-Alonso, C.; Menéndez-Rodríguez, P.; Virgós-Soriano, M.J.; Fernández-Martín, J.L.; Fernández-Coto, M.T.; Cannata-Andía, J.B. Aluminum-Induced Osteogenesis in Osteopenic Rats with Normal Renal Function. *Calcif. Tissue Int.* **1999**, *64*, 534–541, doi:10.1007/S002239900645.
22. Schindelin, J.; Arganda-Carreras, I.; Frise, E.; Kaynig, V.; Longair, M.; Pietzsch, T.; Preibisch, S.; Rueden, C.; Saalfeld, S.; Schmid, B.; et al. Fiji: An Open-Source Platform for Biological-Image Analysis. *Nat. Methods* **2012**, *9*, 676–682, doi:10.1038/nmeth.2019.
23. Görlach, A.; Bertram, K.; Hudecova, S.; Krizanova, O. Calcium and ROS: A Mutual Interplay. *Redox Biol.* **2015**, *6*, 260–271, doi:10.1016/j.redox.2015.08.010.
24. Amberg, G.C.; Navedo, M.F. Calcium Dynamics in Vascular Smooth Muscle. *Microcirculation* **2013**, *20*, 281–289, doi:10.1111/micc.12046.

25. Huang, M.; Zheng, L.; Xu, H.; Tang, D.; Lin, L.; Zhang, J.; Li, C.; Wang, W.; Yuan, Q.; Tao, L.; et al. Oxidative Stress Contributes to Vascular Calcification in Patients with Chronic Kidney Disease. *J. Mol. Cell. Cardiol.* **2020**, *138*, 256–268, doi:10.1016/j.yjmcc.2019.12.006.
26. Watanabe, S.; Fujii, H.; Kono, K.; Watanabe, K.; Goto, S.; Nishi, S. Influence of Oxidative Stress on Vascular Calcification in the Setting of Coexisting Chronic Kidney Disease and Diabetes Mellitus. *Sci. Rep.* **2020**, *10*, doi:10.1038/s41598-020-76838-0.
27. Liberman, M.; Bassi, E.; Martinatti, M.K.; Lario, F.C.; Wosniak, J.; Pomerantzeff, P.M.A.; Laurindo, F.R.M. Oxidant Generation Predominates around Calcifying Foci and Enhances Progression of Aortic Valve Calcification. *Arterioscler. Thromb. Vasc. Biol.* **2008**, *28*, 463–470, doi:10.1161/ATVBAHA.107.156745.
28. Burtenshaw, D.; Hakimjavadi, R.; Redmond, E.M.; Cahill, P.A. Nox, Reactive Oxygen Species and Regulation of Vascular Cell Fate. *Antioxidants* **2017**, *6*, doi:10.3390/antiox6040090.
29. Takaishi, K.; Kinoshita, H.; Kawashima, S.; Kawahito, S. Human Vascular Smooth Muscle Function and Oxidative Stress Induced by Nadph Oxidase with the Clinical Implications. *Cells* **2021**, *10*, doi:10.3390/cells10081947.